PERGAMON Computers and Mathematics with Applications 45 (2003) 699–707

An International Journal
computers & mathematics
with applications

www.elsevier.com/locate/camwa

Third-Order Moment Spectrum and Weighted Fuzzy Classifier for Robust 2-D Object Recognition

SOOWHAN HAN
Department of Multimedia Engineering, Dongeui University
Pusan, South Korea, 614-714
swhan@dongeui.ac.kr

SEUNGJU JANG AND YOUNGWOON WOO
Department of Computer Engineering, Dongeui University
Pusan, South Korea, 614-714

JUNGSIK LEE
School of Electronics and Information Engineering, Kunsan National University
Kunsan, South Korea, 573-701

(Received June 2001; accepted March 2002)

Abstract—In this paper, a robust position, scale, and rotation invariant system for the recognition of closed 2-D noise corrupted images using the bispectral features of a contour sequence and the weighted fuzzy classifier are derived. The higher-order spectrum based on third-order moment, called a bispectrum, is applied to the contour sequences of an image to extract a 15-dimensional feature vector for each of the 2-D images. This bispectral feature vector, which is invariant to shape translation, scale, and rotation transformation, can be used to represent a 2-D planar image and is fed into a weighted fuzzy classifier for the recognition process. The experiments with eight different shapes of aircraft images are presented to illustrate the high performance of the proposed system even when the image is significantly corrupted by noise.

Keywords—Third-order moment spectrum, Bispectrum, Weighted fuzzy mean, Robust object recognition.

1. INTRODUCTION

The studies in 2-D object recognition systems have broad applications such as satellite image identification, the characterization of biomedical images, and the recognition of industrial parts by robots for product assembly. Most of these shape recognition systems require an object to be classified in situations where the position, orientation, and distance of the object are time-varying. Additionally, the systems required to be tolerant to noisy shapes result from the segmentation of objects in varying backgrounds as well as nonideal imaging conditions. There have been over a dozen prior research efforts to improve the performance of systems including Fourier descriptors [1], autoregressive modeling methods [2–4], dynamic alignment process of

0898-1221/03/$ - see front matter Typeset by $\mathcal{A}\mathcal{M}\mathcal{S}$-TEX
PII: S0898-1221(03)00029-4

contour sequences [5], and neural network approaches [6–10]. For the construction of a 2-D object recognition system with high accuracy, while keeping a simplicity of the overall system, two important factors should be considered.

One is to extract a feature vector representing a 2-D object image. The feature vector should have a small dimensionality for real-time process, a similarity between intraclass. In this study, the boundary of a closed planar shape is characterized by an ordered sequence that represents the Euclidean distance between the centroid and all boundary pixels since the overall shape information is contained in the boundary of the shape. After the normalization of this ordered sequence, the bispectrum based on a third-order moment [11,12] is applied as a means of feature extraction. Spectral analyses in most previous works for 2-D object recognition systems were based on power spectrum density, which is the Fourier transform of a second-order moment of contour sequence. However, the power spectrum contains noise power in all the frequency components if the contour sequence is corrupted by white Gaussian noise, where the bispectrum does not. The reason for that and the comparison between two spectra of noisy sequence will be shown in Section 2. Therefore, in our 2-D recognition system, the bispectral components of the normalized contour sequence of an object image are utilized as a feature vector.

Another factor is to select an appropriate classifier architecture for this particular recognition task. The neural network algorithms [6–10] and the fuzzy memberships functions [13,14] are widely used for the recognition classifier. However, the hybrid neural structure with back-propagation and counter-propagation in [8] and with two fuzzy ART modules in [9] are relatively complicated, and the fuzzy ARTMAP in [9] had used the five-voting strategy (repeat five simulations with different ordering of training patterns) to avoid the ordering influence of training patterns. Moreover, in neural network approaches, it is hard to select an optimal neural network architecture for the specific recognition system among many kinds of different neural models [15]. Thus, in this paper, a triangular fuzzy membership function and a weighted fuzzy mean are utilized as a classifier. This fuzzy classifier has a relatively simple structure, and it can easily improve the recognition results by a weighted fuzzy mean extracted from analyzing the bispectral feature vectors. The construction of fuzzy classifier and the recognition process are shown in Section 3.

2. BISPECTRAL FEATURE MEASUREMENT

In this section, the boundary of a closed planar shape is characterized by an ordered sequence that represents the Euclidean distance between the centroid and all contour pixels of the digitized shape. Clearly, this ordered sequence carries the essential shape information of a closed planar image. The bispectral feature extraction from a closed planar image is done as follows. First, the boundary pixels are extracted by using a contour following algorithm and the centroid is derived [16,17]. The second step is to obtain an ordered sequence in a clockwise direction, $b(i)$, that represents the Euclidean distance between the centroid and all boundary pixels. Since only closed contours are considered, the resulting sequential representation is periodic as shown in equation (1).

$$\begin{aligned} b(i) &= \sqrt{(x_i - x_c)^2 + (y_i - y_c)^2}, \qquad \text{and} \\ b(i + PN) &= b(i), \qquad i = 1, 2, 3, \ldots, PN, \end{aligned} \tag{1}$$

where (x_c, y_c) is the centroid of an image, (x_i, y_i) is the contour pixel, and PN (period) is the total number of boundary pixels. This Euclidean distance remains unchanged to a shift in the position of original image. Thus, the sequence $b(i)$ is invariant to translation. The next step is to normalize the contour sequence with respect to the size of the image. Scaling a shape results in the scaling of the samples and duration of the contour sequence. Thus, the scale normalization involves both an amplitude and a duration normalization. The normalized duration of the sequence, 256 points fixed, is obtained by resampling operation and function approximation. This is shown

in equation (2).

$$c(k) = b\left(k * \frac{PN}{256}\right), \qquad k = 1, 2, 3, \ldots, 256, \tag{2}$$

where $c(k)$ is the duration normalized sequence. After duration normalization, the amplitude is divided by the sum of contour sequence and removed the mean. It is shown in equations (3) and (4).

$$d(k) = \frac{c(k)}{s}, \qquad k = 1, 2, 3, \ldots, 256, \tag{3}$$

$$d(k) = d(k) - \text{mean}(d(k)), \tag{4}$$

where $s = c(1)+c(2)+c(3)+\cdots+c(256)$. The sequence $d(k)$ is invariant to translation and scaling. In a fourth step, bispectral feature measurement is taken into the contour sequence. The spectral density of the sequence $d(k)$ is derived by using a third-order moment, called a bispectrum, as mentioned in Section 1. The n^{th}-order moment and its spectrum of contour sequence $d(k)$ are defined as equations (5) and (6), respectively.

$$M_n(\tau_1, \tau_2, \ldots, \tau_{n-1}) = \frac{1}{N}\sum_{k=0}^{N-1} d(k)\, d(k+\tau_1)\cdots d(k+\tau_{n-1}), \tag{5}$$

$$H_n(\lambda_1, \ldots, \lambda_{n-1}) = \sum_{\tau_1=0}^{N-1}\cdots\sum_{\tau_{n-1}=0}^{N-1} M_n(\tau_1, \tau_2, \ldots, \tau_{n-1}) e^{-j(2\pi/N)(\lambda_1\tau_1+\cdots+\lambda_{n-1}\tau_{n-1})}, \tag{6}$$

where N is the length of normalized sequence $d(k)$, 256 in this study. For the special cases where $n = 2$ (power spectrum) and $n = 3$ (bispectrum),

$$\begin{aligned} H_2(\lambda) &= \sum_{\tau=0}^{N-1} M_2(\tau) e^{-j(2\pi/N)\lambda\tau} = \sum_{\tau=0}^{N-1}\frac{1}{N}\sum_{k=0}^{N-1} d(k)\, d(k+\tau)\, e^{-j(2\pi/N)\lambda\tau} \\ &= \sum_{\tau=0}^{N-1}\frac{1}{N}\sum_{k=0}^{N-1} d(k)\, d(k+\tau)\, e^{-j(2\pi/N)\lambda(\tau+k-k)} \\ &= \frac{1}{N}\sum_{\tau=0}^{N-1} d(k+\tau)\, e^{-j(2\pi/N)\lambda(k+\tau)} \sum_{k=0}^{N-1} d(k)\, e^{j(2\pi/N)\lambda k} = \frac{1}{N}F(\lambda)F^*(\lambda), \end{aligned} \tag{7}$$

where $F(\lambda)$ is a Fourier transform of the sequence $d(k)$. In the same way,

$$\begin{aligned} H_3(\lambda_1, \lambda_2) &= \sum_{\tau_1=0}^{N-1}\sum_{\tau_2=0}^{N-1} M_3(\tau_1, \tau_2) e^{-j(2\pi/N)(\lambda_1\tau_1+\lambda_2\tau_2)} \\ &= \sum_{\tau_1=0}^{N-1}\sum_{\tau_2=0}^{N-1}\frac{1}{N}\sum_{k=0}^{N-1} d(k)\, d(k+\tau_1)\, d(k+\tau_2) e^{-j(2\pi/N)(\lambda_1\tau_1+\lambda_2\tau_2)} \\ &= \frac{1}{N}\sum_{\tau_1=0}^{N-1}\sum_{\tau_2=0}^{N-1}\sum_{k=0}^{N-1} d(k)\, d(k+\tau_1)\, d(k+\tau_2) e^{-j(2\pi/N)(\lambda_1(k+\tau_1)+\lambda_2(k+\tau_2)-k(\lambda_1+\lambda_2))} \\ &= \frac{1}{N}\sum_{\tau_1=0}^{N-1} d(k+\tau_1) e^{-j(2\pi/N)\lambda_1(k+\tau_1)} \sum_{\tau_2=0}^{N-1} d(k+\tau_2) e^{-j(2\pi/N)\lambda_2(k+\tau_2)} \\ &\quad \times \sum_{k=0}^{N-1} d(k)\, e^{j(2\pi/N)k(\lambda_1+\lambda_2)} \\ &= \frac{1}{N}F(\lambda_1)F(\lambda_2)F^*(\lambda_1+\lambda_2). \end{aligned} \tag{8}$$

If the observed contour sequence $d(k) = s(k) + n(k)$ where $s(k)$ is the zero mean contour sequence without noise, $n(k)$ is the zero mean white Gaussian noise sequence with $N_0/2$ power and they are independent, equations (7) and (8) become

$$\begin{aligned}
H_2(\lambda) &= \sum_{\tau=0}^{N-1} M_2(\tau) e^{-j(2\pi/N)\lambda\tau} \\
&= \sum_{\tau=0}^{N-1} \frac{1}{N} \sum_{k=0}^{N-1} [(s(k)+n(k))(s(k+\tau)+n(k+\tau))] e^{-j(2\pi/N)\lambda\tau} \\
&= \sum_{\tau=0}^{N-1} \frac{1}{N} \sum_{k=0}^{N-1} s(k)s(k+\tau) e^{-j(2\pi/N)\lambda\tau} + \sum_{\tau=0}^{N-1} \frac{1}{N} \sum_{k=0}^{N-1} n(k)n(k+\tau) e^{-j(2\pi/N)\lambda\tau} \\
&= \frac{1}{N} \sum_{\tau=0}^{N-1} \sum_{k=0}^{N-1} s(k)s(k+\tau) e^{-j(2\pi/N)\lambda\tau} + \sum_{\tau=0}^{N-1} \frac{N_0}{2} \delta(\tau) e^{-j(2\pi/N)\lambda\tau} \\
&= \frac{1}{N} F_s(\lambda) F_s^*(\lambda) + \frac{N_0}{2} = H_s(\lambda) + H_n(\lambda).
\end{aligned} \tag{9}$$

$$\begin{aligned}
H_3(\lambda_1, \lambda_2) &= \sum_{\tau_1=0}^{N-1} \sum_{\tau_2=0}^{N-1} M_3(\tau_1, \tau_2) e^{-j(2\pi/N)(\lambda_1\tau_1 + \lambda_2\tau_2)} \\
&= \sum_{\tau_1=0}^{N-1} \sum_{\tau_2=0}^{N-1} \frac{1}{N} \sum_{k=0}^{N-1} [(s(k)+n(k))(s(k+\tau_1)+n(k+\tau_1)) \\
&\quad \times (s(k+\tau_2)+n(k+\tau_2))] e^{-j(2\pi/N)(\lambda_1\tau_1 + \lambda_2\tau_2)} \\
&= \sum_{\tau_1=0}^{N-1} \sum_{\tau_2=0}^{N-1} \frac{1}{N} \sum_{k=0}^{N-1} s(k)s(k+\tau_1)s(k+\tau_2) e^{-j(2\pi/N)(\lambda_1\tau_1 + \lambda_2\tau_2)} \\
&\quad + \sum_{\tau_1=0}^{N-1} \sum_{\tau_2=0}^{N-1} \frac{1}{N} \sum_{k=0}^{N-1} n(k)n(k+\tau_1)n(k+\tau_2) e^{-j(2\pi/N)(\lambda_1\tau_1 + \lambda_2\tau_2)} \\
&= \frac{1}{N} \sum_{\tau_1=0}^{N-1} \sum_{\tau_2=0}^{N-1} \sum_{k=0}^{N-1} s(k)s(k+\tau_1)s(k+\tau_2) e^{-j(2\pi/N)(\lambda_1\tau_1 + \lambda_2\tau_2)} \\
&\quad + \sum_{\tau_1=0}^{N-1} \sum_{\tau_2=0}^{N-1} \gamma_n \delta(\tau_1, \tau_2) e^{-j(2\pi/N)(\lambda_1\tau_1 + \lambda_2\tau_2)} \\
&= \frac{1}{N} F_s(\lambda_1) F_s(\lambda_2) F_s^*(\lambda_1 + \lambda_2) + \gamma_n = H_s(\lambda_1, \lambda_2) + H_n(\lambda_1, \lambda_2),
\end{aligned} \tag{10}$$

where γ_n is a skewness of $n(k)$, $H(\lambda)$ and $H_n(\lambda)$ are the power spectrum, and $H_s(\lambda_1, \lambda_2)$ and $H_n(\lambda_1, \lambda_2)$ are the bispectrum of $s(k)$ and $n(k)$, respectively. By equation (9), the power spectrum contains the noise power, $N_0/2$, in all frequency ranges. However, the bispectrum of $n(k)$ in equation (10), $H_n(\lambda_1, \lambda_2) = \gamma_n$, becomes zero because of the symmetric property of noise density function, which means the bispectrum suppresses the white noise portion, and the extracted feature vector from the bispectrum space has better noise tolerance than the feature vector from the power spectrum space. The variations of 15-dimensional feature values for each reference image, based on power spectrum and bispectrum space with 25 db and 10 db SNR, were calculated by equation (11) and shown in Table 1.

$$\text{VA(Variation)} = E\left[\left(\frac{\text{FF} - \text{FN}}{\text{FF}}\right)^2\right], \tag{11}$$

where FF and FN are the 15-dimensional feature values extracted from the reference image (noise free) and noise corrupted image, respectively. VA for bispectrum under 10 db SNR in Table 1

Table 1. The variations of features extracted from PS (power spectrum) and BS (bispectrum) of noise corrupted sequence $d(k)$.

Reference Images (a_1–a_8) in Figure 3		a_1	a_2	a_3	a_4	a_5	a_6	a_7	a_8
SNR: 25 db	VA for PS	0.07	0.14	0.02	0.05	0.08	0.20	0.29	0.25
SNR: 25 db	VA for BS	0.02	0.08	0.01	0.01	0.02	0.04	0.04	0.01
SNR: 10 db	VA for PS	26.07	66.74	27.10	35.11	151.18	49.24	21.71	179.60
SNR: 10 db	VA for BS	1.04	3.37	1.28	1.88	2.9	5.6	0.41	4.49

is relatively smaller, which means the bispectral feature vector is not significantly influenced by noise. Therefore, the bispectrum was utilized for feature selection of 2-D shape images in this paper. More details for the performance analysis between two spectral features can be found in [10]. The magnitude of bispectrum derived in a fourth step, $|H(\lambda_1, \lambda_2)|$, is unchanged even after the sequence $d(k)$ is circular shifted because the magnitude of Fourier transform, $|F(\lambda)|$, is not changed [18]. Thus, $|H(\lambda_1, \lambda_2)|$ is invariant to the rotation of an image. Finally, the two-dimensional bispectral magnitudes (256 by 256) are projected to vertical axis (λ_1) by taking the mean value of each column for feature extraction. It is shown in equation (12).

$$h(k) = \text{mean of } k^{\text{th}} \text{ column of } |H(\lambda_1, \lambda_2)|, \tag{12}$$

where $k = 1, 2, \ldots, 256$. The first column and row in the magnitude of bispectrum contain all zero values because the normalized contour sequence $d(k)$ has a zero mean. It means $h(1)$ is always zero. And the projected bispectral components exceeded to the 16^{th} have very small values (near zero). Thus, for fast recognition process with reliable accuracy, the projected bispectral components from the second to the 16^{th} $(h(2), h(3), \ldots, h(16))$ are chosen to be used as feature values to represent each image shape, which are fed into a proposed weighted fuzzy classifier for recognition process. These feature vectors have the desired format for a planar image recognition system, which means they are invariant to translation and rotation and scaling of the shape, and highly tolerant to the noise. The overall bispectral feature extraction process is shown in Figure 1.

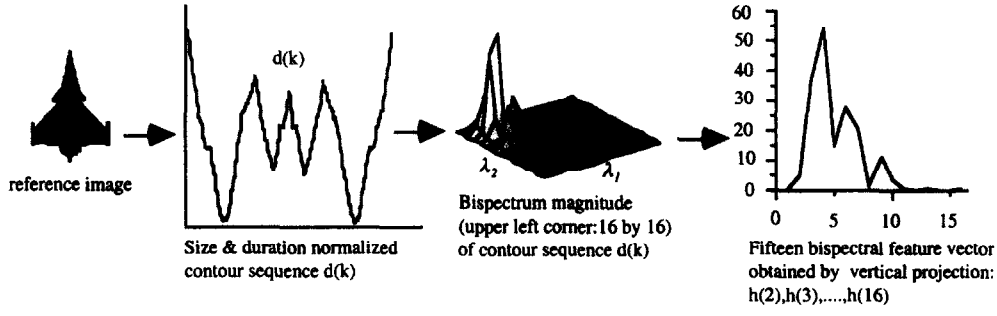

Figure 1. The overall processing step for bispectral feature extraction.

3. CONSTRUCTION OF A WEIGHTED FUZZY CLASSIFIER AND RECOGNITION PROCEDURE

The construction of a fuzzy classifier and the recognition process are done as follows. First, the 15 fuzzy membership functions for each of the reference aircraft images are established by using 15-dimensional bispectral feature values of the reference feature set. The fuzzy membership functions are defined by equations (13) and (14).

$$\begin{aligned} \mu_{ij}(x_i) &= \frac{x_i - f_{ij}}{100} + 1, \qquad \text{if } x_i < f_{ij}, \qquad \text{and} \\ \mu_{ij}(x_i) &= -\frac{x_i - f_{ij}}{100} + 1, \qquad \text{if } x_i \geq f_{ij}, \end{aligned} \tag{13}$$

$$\mu_{ij}(x_i) = \begin{cases} \mu_{ij}(x_i), & \text{if } \mu_{ij}(x_i) \geq 0, \\ 0, & \text{if } \mu_{ij}(x_i) < 0, \end{cases} \tag{14}$$

where 0.01 is the selected slope of a fuzzy membership function, x_i is an i^{th} feature value of input aircraft image, f_{ij} is an i^{th} feature value of reference feature set for an image a_j, and $\mu_{ij}(x_i)$ is a membership grade for x_i. All membership functions are configured as a triangular type shown in Figure 2, and the total number of fuzzy membership functions in this process becomes 120 (15×8: the one membership function for each of 15-dimensional reference feature values $\times$ eight different aircraft images shown in Figure 3).

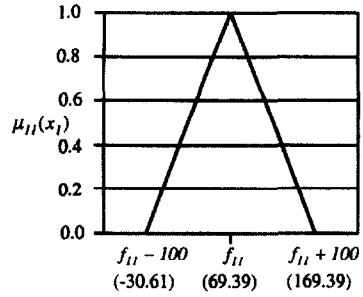

Figure 2. Fuzzy membership grade function for the first bispectral feature value extracted from image a_1 shown in Figure 3.

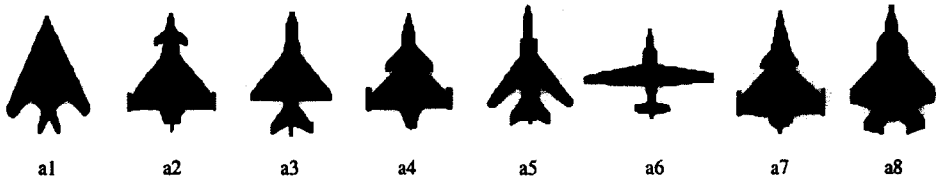

Figure 3. Eight different shapes of reference aircraft images.

Next, the variances of each of the 15-dimensional feature values in the reference feature set are derived after normalization. They are shown in equation (15) for normalization and in equation (16) for variances. Those variances are utilized as the weights for the recognition process.

$$\text{nf}_{ij} = \frac{f_{ij}}{\sum_{j=1}^{8} f_{ij}}, \qquad i = 1, 2, \ldots, 15, \tag{15}$$

where f_{ij} is an i^{th} feature value of reference feature set for an image a_j, and nf_{ij} is a normalized i^{th} reference feature value for an image a_j.

$$\text{vr}_i = \frac{1}{8} \sum_{j=1}^{8} (\text{nf}_{ij} - m_i)^2, \qquad i = 1, 2, \ldots, 15, \tag{16}$$

where m_i is a mean of nf_{ij} for eight different reference images ($j = 1, 2, \ldots, 8$) and vr_i is its variance.

In the recognition process, the 15-dimensional bispectral feature values of an incoming test image are applied to the corresponding fuzzy membership functions of the reference feature set for each of eight different aircraft images, and the membership grades are computed by equations (13) and (14). These 15 membership grades with each of eight reference feature sets present the degree of similarity with each of eight different aircraft images. Finally, the variances shown in equation (16) are utilized as weights, and the weighted fuzzy mean values of the membership grades are computed by equation (17). Any one of eight reference sets with the largest weighted

fuzzy mean value is selected as a recognition result for an incoming test image. By using the weights shown in equation (17), a membership grade of the i^{th} feature value which is significantly different between eight aircraft images is more emphasized during the recognition process.

$$h_j(\mu_{1j}(x_1), \mu_{2j}(x_2), \ldots, \mu_{15j}(x_{15});\ w_1, w_2, \ldots, w_{15}) = \sum_{i=1}^{15} \mu_{ij}(x_i) \cdot w_i, \qquad j = 1, 2, \ldots, 8, \quad (17)$$

where h_j and μ_{ij} are a weighted fuzzy mean value and a membership grade of the i^{th} feature value for an aircraft image a_j $(j = 1, 2, \ldots, 8)$, respectively, and $w_i = vr_i$ $(i = 1, 2, \ldots, 15)$. In cases without weights, h_j is simply a sum of membership grades of the 15-dimensional bispectral feature values shown in equation (18).

$$h_j(\mu_{1j}(x_1), \mu_{2j}(x_2), \ldots, \mu_{15j}(x_{15})) = \sum_{i=1}^{15} \mu_{ij}(x_i). \quad (18)$$

During the recognition process using h_j in equation (18), all of the 15-dimensional feature values are equally weighted even though some of them might have a unique difference to distinguish between eight aircraft images.

4. EXPERIMENTAL RESULTS

The methodology presented in this paper, for the recognition of a closed planar shape, was evaluated with eight different shapes of aircraft. They are shown in Figure 3. From each reference shape of aircraft, 36 noise-free patterns were generated by rotating the original image with 30 degree increment and scaling with three factors (1, 0.8, and 0.6). And 40 noise corrupted patterns were made by adding four different levels of random Gaussian noise (25 db, 20 db, 15 db, 10 db SNR: ten noisy patterns for each SNR) to 36 noise-free patterns. The sample contour images with 5 db SNR shown in Figure 4 are heavily corrupted by noise, and the recognition process seems to be meaningless. That is why the images with less than 10 db SNR are not included in our experimental process. Thus, the data set for each reference aircraft image has 36 noise-free patterns and 1440 (40×36) noise corrupted patterns. The number of total test patterns becomes 11808 $(1476 \times 8$ reference images).

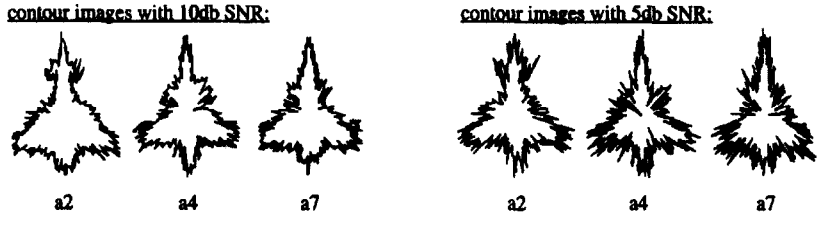

Figure 4. Some contour images with low level SNR.

The recognition process was carried out under three different experimental environments depending on the configuration of reference feature sets for fuzzy membership function. These are as follows.

REFERENCE FEATURE SET 1. Bispectral feature vectors extracted from only the eight reference images shown in Figure 3.

REFERENCE FEATURE SET 2. Averaged bispectral feature vectors extracted from eight reference images + 32 noisy patterns (four noisy patterns with 25 db SNR from each of eight reference images).

REFERENCE FEATURE SET 3. Averaged bispectral feature vectors extracted from eight reference images + 32 noisy patterns (four noisy patterns with each one of 25 db, 20 db, 15 db, and 10 db SNR from each of eight reference images).

All 11808 test images were evaluated by a fuzzy classifier with weights and without weights for each of three different reference feature sets. In the experiments with reference Feature Sets 2 and 3, five independent simulations were performed with a different choice of noisy patterns for the configuration of a reference feature set, and the classification results were averaged. They are summarized in Table 2. It shows that the results with reference feature set configured by more various types of noisy patterns, such as Feature Set 3, are better than the results with reference feature sets by only the eight noise-free patterns (Feature Set 1) or limited noisy patterns (Feature Set 2). It is known that the classification results of a fuzzy classifier can be increased by adding some noisy patterns to the construction of reference feature set. And both of two fuzzy classifiers with and without weights recognize well the eight different shapes of images where the signal power is relatively larger than the noise power (in case of noise-free, 25 db, 20 db, 15 db). However, the experimental results with 10 db SNR show that the fuzzy classifier with weights is more effective where the images are highly corrupted by noise. It means the weighted fuzzy mean shown in equation (17) has a better noise tolerance than the simple sum of membership grades shown in equation (18). And most errors with 10 db SNR were caused by the misclassification between images a_4 and a_7. The reason for that can be found in Figure 4, which shows the similarity of two images with low level SNR. From the averaged misclassification errors between a_4 and a_7 vs. total number of errors shown in Table 3, it is known that the use of weights can help to reduce the misclassification between two similar images. In the best result with reference Feature Set 3, only 12 patterns were misclassified among 11808 test patterns, and the classification ratios reached almost 100%. The overall averaged classification results for a weighted fuzzy classifier with all three different reference feature sets were obtained over 99%. These experimental results say the bispectral feature vectors with the weighted fuzzy classifier have the acceptable discrimination ability between each aircraft pattern even when the patterns were significantly corrupted by noise.

Table 2. The averaged classification results with four different noise levels.

	Reference Set 1: with Weights (without Weights)	Reference Set 2: with Weights (without Weights)	Reference Set 3: with Weights (without Weights)
Noise-free: 8 × 3 (scale) × 12 (rotation)	288/288 : 100% (288/288 : 100%)	288/288 : 100% (288/288 : 100%)	288/288 : 100% (288/288 : 100%)
25 db: 288 × 10 (noise patterns)	2880/2880 : 100% (2880/2880 : 100%)	2880/2880 : 100% (2880/2880 : 100%)	2880/2880 : 100% (2880/2880 : 100%)
20 db: 288 × 10 (noise patterns)	2880/2880 : 100% (2880/2880 : 100%)	2880/2880 : 100% (2880/2880 : 100%)	2880/2880 : 100% (2880/2880 : 100%)
15 db: 288 × 10 (noise patterns)	2880/2880 : 100% (2880/2880 : 100%)	2880/2880 : 100% (2880/2880 : 100%)	2880/2880 : 100% (2880/2880 : 100%)
10 db: 288 × 10 (noise patterns)	2806/2880 : 97.43% (2760/2880 : 95.83%)	2814/2880 : 97.71% (2771/2880 : 96.22%)	2859/2880 : 99.27% (2850/2880 : 98.96%)
Total num. of correctly classified patterns (%)	11734/11808 : 99.37% (11688/11808 : 98.98%)	11742/11808 : 99.44% (11699/11808 : 99.08%)	11787/11808 : 99.82% (11778/11808 : 99.75%)

Table 3. The averaged misclassification ratios between images a_4 and a_7 with 10 db SNR.

	Reference Set 1: with Weights (without Weights)	Reference Set 2: with Weights (without Weights)	Reference Set 3: with Weights (without Weights)
Num. of errors between a_4 and a_7 ÷ total num. of errors	24/74 : 32.43% (82/120 : 68.33%)	23/66 : 34.85% (72/109 : 66.06%)	6/21 : 28.57% (18/30 : 60.00%)

5. CONCLUSION

The high classification results in experimental process show that the weighted fuzzy classifier with the 15-dimensional bispectral feature vectors extracted from the normalized contour sequences of images performs well in recognizing the different shapes of aircraft images even when the images are rotated, scaled, and significantly corrupted by noise. Additionally, the classification results are easily improved by using the weights extracted from analyzing the feature values, and the overall processing step is relatively simple. For this type of fuzzy classifier, the training period is not required because the reference feature set can be simply constructed with some image samples. For practical applications, further research in the near future should involve the experiments with more realistic data such as satellite images or biomedical images. And at the same time, the way to segment the shape of image from noisy background should be considered for real world applications.

REFERENCES

1. C.C. Lin and R. Chellappa, Classification of partial 2-D shapes using Fourier descriptors, *IEEE Trans. on PAMI* **9** (5), 686–690, (September 1987).
2. S.R. Dubois and F.H. Glanz, Autoregressive model approach to two-dimensional shape classification, *IEEE Trans. on PAMI* **8** (1), (January 1986).
3. I. Sekita, T. Kurita and N. Otsu, Complex autoregressive model for shape recognition, *IEEE Trans. on PAMI* **14** (4), (April 1992).
4. M. Das, M.J. Paulik and N.K. Loh, A bivariate autoregressive modeling technique for analysis and classification of planar shapes, *IEEE Trans. on PAMI* **12** (1), (January 1990).
5. L. Gupta and M.D. Srinath, Invariant planar shape recognition using dynamic alignment, *Pattern Recognition* **21** (3), 235–239, (1988).
6. L. Gupta, M.R. Sayeh and R. Tammana, A neural network approach to robust shape classification, *Pattern Recognition* **23** (6), 563–568, (1990).
7. L. Spirkovska and M.B. Reid, Robust position, scale, and rotation invariant object recognition using higher-order neural networks, *Pattern Recognition* **25** (9), 975–985, (1992).
8. B.H. Cho, Rotation, translation and scale invariant 2-D object recognition using spectral analysis and a hybrid neural network, Ph.D. Thesis, Florida Institute of Technology, Melbourne, FL, (1993).
9. S.W. Han, Robust planar shape recognition using spectrum analyzer and fuzzy artmap, *Korea Journal of Fuzzy Logic and Intelligent Systems* **5** (4), 33–40, (June 1997).
10. S.W. Han, A study on 2-D shape recognition using higher-order spectral and LVQ, *Korea Journal of Fuzzy Logic and Intelligent Systems* **9** (3), 285–293, (June 1999).
11. C.L. Nikias and M.R. Raghuveer, Bispectrum estimation: A digital signal processing framework, *Proc. IEEE* **75** (7), 869–891, (July 1987).
12. C.L. Nikias and J.M. Mendel, *Signal Processing with Higher-Order Spectra*, United Signals & Systems, (1990).
13. A. Kandel, *Fuzzy Techniques in Pattern Recognition*, John Wiley & Sons, (1982).
14. H.J. Zimmermann, *Fuzzy Set Theory—And Its Applications*, pp. 217–239, Kluwer Academic, (1996).
15. L. Fausett, *Fundamentals of Neural Networks: Architectures, Algorithm, and Applications*, Prentice-Hall, (1994).
16. R.C. Gonzalez and R.E. Woods, *Digital Image Processing*, Addison-Wesley, (1992).
17. W.K. Patt, *Digital Image Processing*, Second Edition, Wiley Interscience, (1991).
18. A.V. Oppenheim and R.W. Schafer, *Digital Signal Processing*, Prentice-Hall, Englewood Cliffs, NJ, (1975).